Scanning Electrochemical Cell Microscopy: A Natural Technique for Single Entity Electrochemistry

Oluwasegun J. Wahab, Minkyung Kang*, Patrick R. Unwin*

Department of Chemistry, University of Warwick, Coventry CV4 7AL, U.K.

Corresponding authors: * minkyung.kang@warwick.ac.uk and *p.r.unwin@warwick.ac.uk

Abstract

Scanning electrochemical cell microscopy (SECCM) is a robust and versatile scanning electrochemical probe microscopy technique that allows direct correlation of structure-activity at the nanoscale. SECCM utilizes a mobile droplet cell to investigate and visualize electrochemical activity at interfaces with high spatio-temporal resolution, while also providing topographical information. This article highlights diverse contemporary challenges in the field of single entity electrochemistry (SEE) tackled by the increasing uptake of SECCM globally. Various applications of SECCM in SEE are featured herein, including electrocatalysis, electrodeposition, corrosion science and materials science, with electrode materials spanning particles, polymers, 2D materials and complex polycrystalline substrates. The use of SECCM for patterning structures is also highlighted.

1.0 Introduction

Single entity electrochemistry (SEE) is an exciting and rapidly evolving field focused on characterizing the electrochemical properties of "things" [1]. The *thing* represents a simple unit (nano- to microscale) of a more complex system, such as a particle, nanotube or nanopore, or an elementary feature of a complex surface, such as a step site, terrace or region of particular surface chemistry. Understanding the electrochemical characteristics of single entities reveals their unique contributions to the ensemble 'averaged' macroscopic response of an electrode or electro-material, and opens up the prospect of elucidating the interactions between entities. SEE, therefore, presents a means to grasp the uniqueness and complexity of electrode and electro-material systems from a "bottom-up" perspective.

SEE is challenging experimentally because it usually requires the use of nanoscale probes/electrodes and measurement of low signals with the best time resolution possible, while making repetitive measurements over multiple (different) individual entities to build informative statistical databases and deconstruct the macroscopic view [1–3]. This article considers the attributes and expanding applications of scanning electrochemical cell microscopy (SECCM), a (nano)pipet-based technique [4–6].

In SECCM, a mobile meniscus (electrochemical) cell or half-cell is brought into contact with the target entity (surface), by implementing an electrochemical feedback protocol (Figure 1A and B). Then, the electrochemical measurement of interest takes place locally. As a scanning tool, arrays of measurements are possible either by a constant distance or hopping scanning regime (Figure 1C and D). In the hopping scanning regime, which can be deployed with various electrochemical methods, the meniscus is completely detached from the surface after each measurement then re-positioned to an adjacent area without overlapping previously

contacted area. This makes it highly robust and versatile, as the contacted area (droplet footprint) is well defined and can often be visualized and measured after experiments, e.g. by scanning electron microscopy, to allow precise knowledge of the size of the electrochemical cell formed between the nanopipet meniscus and the surface. A general advantage of hopping mode in scanning probe microscopy is that features on rough surfaces are more readily addressed with greatly reduced risk of tip crash (Figure 1D) [7–9]. Details on the operational principles of SECCM have been extensively detailed elsewhere [10,11].

While the main studies to date have considered constant potential [12] and voltammetric imaging [13], current-time and chronopotentiometric measurements are also feasible [14]. The growth and applications of SECCM in the past few years has been fueled by the increasing availability of instrumentation, which is available freely on request from our group [11] and several groups have also built their own instruments [15–18]. This article provides a survey of the most recent SEE studies explored with SECCM, and further provides a brief view of trans-disciplinary opportunities awaiting exploitation.

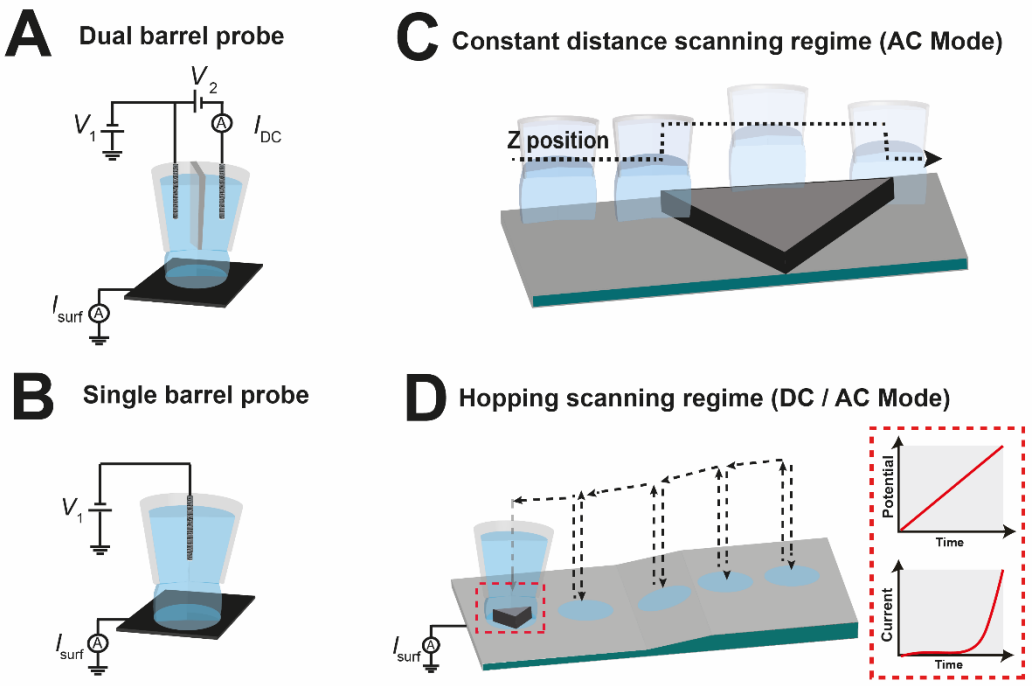

Figure 1: Schematic of scanning electrochemical cell microscopy (SECCM) probes and setup for voltammetry and amperometry. Dual (A) and single (B) barrel probes (micro- or nanopipets) filled with electrolyte and quasi-reference counter electrode(s), QRCE(s), are used as scanning probes in SECCM. The single barrel probes can be used for conductive surfaces (electrodes) while dual barrel probes are also applicable to insulating surfaces. With dual barrel probes, the direct ion current (I_{DC}) across the meniscus, with a potential bias between two barrels (V_2), is monitored for positioning. Upon droplet contact with the surface, there is a change in I_{DC}. The potential V_1 sets the driving force for electrochemical reactions and the working electrode current (I_{surf}) is measured. The dual barrel probe can also be modulated vertically at a set frequency, using a sinusoidal signal from a lock-in amplifier, and the resulting AC signal used for positioning. Schematic of the probe transit in (C) for the constant distance scanning regime and (D) hopping scanning regime over a nanocrystal on a support (not to scale). Inset in (D) shows the potential-time waveform for linear sweep voltammetry and the resulting current response recorded at each meniscus landing (image pixel).

2.0 Expansive Single Entity Applications of SECCM

2.1 Electrocatalysis at pseudo-single crystal electrodes and grain boundaries

The pseudo-single crystal approach with SECCM [19] offers a means of screening multiple crystallographic orientations and grain boundaries (GBs) on a polycrystalline metal surface. The surface region of interest is often characterized with electron backscatter diffraction (EBSD) to correlate with SECCM data (Figure 2). Recent applications include determination of how local boron dopant level and surface terminations (oxygen or hydrogen), within the same crystal orientation, govern the solvent window of conductive boron-doped diamond (BDD) [20]. In a separate example, higher rates of electrochemical hydrogen absorption at annealed polycrystalline Pd were shown to be facilitated by high-index grain orientations and GBs, compared to low-index orientations [21].

H_2 gas nucleation during hydrogen evolution reaction (HER), studied extensively with nanoelectodes [22], was spatially resolved on a polycrystalline Pt surface [23] through voltammetric SECCM [13]. The adoption of this approach has further enabled the measurement of nanobubble nucleation from HER and correlation with the potential of zero charge (PZC) on polycrystalline Pt surfaces [24]. For PZC measurements, the SECCM nanopipet was repetitively approached to each point on the surface at a series of potentials, and the resulting charge *vs.* potential plots at each point allowed the direct extraction of local PZC, for correlation with the crystallographic orientation (Figure 2A-C) [24]. This work elucidated the relationship between PZC (from which the work function was determined) and grain-dependent HER activity.

SECCM with environmental control [11], has been used to investigate GB electrochemistry at polycrystalline Au electrodes [25], showing that electrocatalytically active GBs on Au

electrodes selectively enhance CO_2 reduction to CO, in proportion to the strain field/dislocation density (Figure 2D and E). These works highlight the considerable contribution of SECCM pseudo-single crystal measurements that provides a road map to identify and design optimal (electro)catalysts.

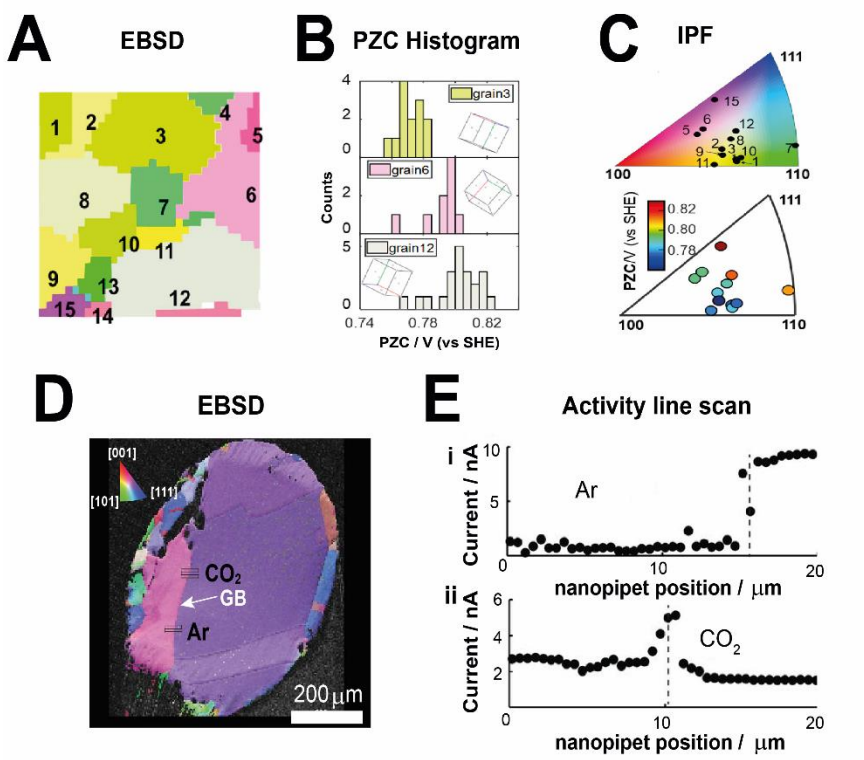

Figure 2: Grain-dependent and grain boundary (GB) electrochemical characteristics from SECCM. (A-C) Mapping local potential of zero charge (PZC). (A) Electron backscatter diffraction (EBSD) map of an SECCM scan area with the locations of 15 measurements, 3 of which are shown in (B). (C) Crystal orientations (top) and average PZC values (bottom) of each of the 15 areas as an inverse pole figure (IPF). Adapted with permission from reference [24]. Copyright 2020 American Chemical Society. (D and E) Local CO_2 electroreduction measurements at GBs on polycrystalline Au. (D) EBSD map of Au wire showing the path of 2 sets of SECCM line scans across a GB in Ar and CO_2. (E) SECCM line scan for HER in Ar (top) and CO_2 reduction (bottom). Dashed lines indicate the position of GBs. From reference [25]. Reprinted with permission from AAAS.

2.2 Corrosion and Films

SECCM has recently expanded into corrosion-related measurements with high spatio-temporal resolution [9,16,26–28]. The anodic passivation of low carbon steel [26] was analyzed using voltammetric SECCM with the pseudo-single crystal approach of Section 2.1. Among the low index planes, corrosion susceptibility was highest on (101) planes compared to (111) and (100) planes in neutral electrolyte solution. Tafel analysis, supported by complementary multi-microscopy characterization, additionally revealed unique electrochemical behavior of individual sub-micron MnS inclusions on the low carbon steel surface. Nanopipets with diameter of ~150 nm enabled direct nanoscopic electrochemical characterization of the HER at low carbon steel in sulfuric acid (pH 2.3) [9]. HER activity was in the order {100} > {111} > {101} and some GB termination and MnS inclusions (*ca.* 100 nm) were identified as highly active cathodic sites (Figure 3A-C). In a similar study of polycrystalline Zn in acidic media indicated that both HER (cathodic) and Zn electrodissolution (anodic) on low-index grains decreased in order $(\bar{1}2\bar{1}0) \geq (01\bar{1}0) > (0001)$ [28].

More complex corrosion processes, including Fe dissolution, were further studied on low carbon steel in acid media using SECCM, together with cross-sectional scanning transmission electron microscopy (csSTEM) and electron dispersive spectroscopy (EDS) [27]. Co-located EBSD analysis confirmed that anodic dissolution rates of Fe increased in the order {100} > {111} > {101}. Further, the composition and structure of local corrosion products, electrochemically induced by SECCM, were fully characterized by csSTEM and EDS, highlighting advantages of *correlative electrochemical multi-microscopy* in corrosion research.

Another important aspect of corrosion studies is the characterization of passive films. In this context, the use of voltammetric SECCM with ferrocenemethanol oxidation for the identification of pinhole defects in passivating aryl films formed on glassy carbon electrode [16] is an interesting advance. Aided by numerical simulation, sensitivity towards the detection of pinholes of ≤ 10 nm size was achieved with 500 nm-sized nanopipets. SECCM has also been applied to study a Mg-Al diffusion (metal) couple, in order to monitor the corrosion behavior at the solid/solid interfaces with different metal composition [29].

2.3 Single particles studies

SECCM is particularly attractive for single nanoparticle (NP) studies, whereby the electrochemistry of individual NPs within an ensemble can be measured and correlated with the structure or morphology obtained from co-located complementary surface analysis [12,30]. This capability is of crucial importance, because individual NPs within a synthesized batch can show a range of subtle structural differences which will influence the chemical and physical properties [31] and would be expected to affect electrochemistry at the single NP level. Various electrocatalytic reactions have been explored on single particles with SECCM, including HER, oxygen evolution reaction (OER), oxygen reduction reaction (ORR) and hydrazine oxidation [15,17,32,33]. Voltammetric measurements on individual zeolite imidazolate framework derived nanocomposites (e.g., Co-N-doped C) revealed that the "apparent" (electro)catalytic OER activity is proportional to both the number and size of particles encapsulated in droplet cell [32].

Combining rational nanomaterial design with single NP electrochemistry enables in-depth correlative structure−activity investigations. Cubic and octahedral faceted Au nanocrystals (CNs and ONs, respectively) engineered to expose predominantly {100} and {111},

respectively (population of 200), were individually studied for HER activity [15]. CNs were shown to have higher activity for HER compared to ONs (Figure 3D-F) [34]. Significantly, there were variations between crystals of the same morphology (Figure 3E), highlighting the importance of SEE measurements to reveal activity distributions within a population of particles. By combining SECCM with optical hyperspectral imaging, the spatial locations of NPs of interest (Au nanorods) on an electrode support were determined for targeted electrochemical measurements [17]. This new approach, moreover, opens up the prospect of future in situ electrochemical and spectroscopic investigations in SEE.

A key attribute of SECCM is that the working electrode, with which the meniscus makes contact, can have a wide range of forms, including TEM grids [30,35]. Pt NPs with a narrow size distribution (average diameter of ~3 nm) deposited onto a carbon-coated TEM grid, were investigated to understand the interactions between the electrocatalysts and the supporting electrodes during the ORR [33]. The effect of NP coverage on the extent of surface poisoning due to corrosion of the support by peroxy-intermediates was elucidated. In some circumstances, high mobility of Pt NPs was also observed due to uneven oxygen fluxes to individual NPs within an ensemble, resulting in NPs adopting characteristic patterns on the TEM grid after ORR.

SECCM is also powerful for studying energy storage materials at the SEE level as illustrated by several studies of cathode materials for lithium ion battery (LIB) [36–38]. To move SECCM beyond aqueous systems, an ionic liquid can be used as the electrolyte solution in SECCM, which extends the potential window and increases droplet stability [36,39]. SECCM with ionic liquid was utilized to electrochemically characterize an ensemble of $LiFePO_4$ nanocomposites dispersed on glassy carbon, successfully examining Li-ion (de)intercalation [36]. Employing

both cyclic voltammetric and galvanostatic modes, Li-ion (de)intercalation and charge-discharge profiles of single $LiMn_2O_4$ NPs revealed heterogeneity in electrochemical behavior of apparently similar particles based on their size, composition, crystallinity and orientation [37]. This work further suggested that orders of magnitude faster charge-discharge rates can be achieved at the single particle level compared to composite electrodes at the macroscale.

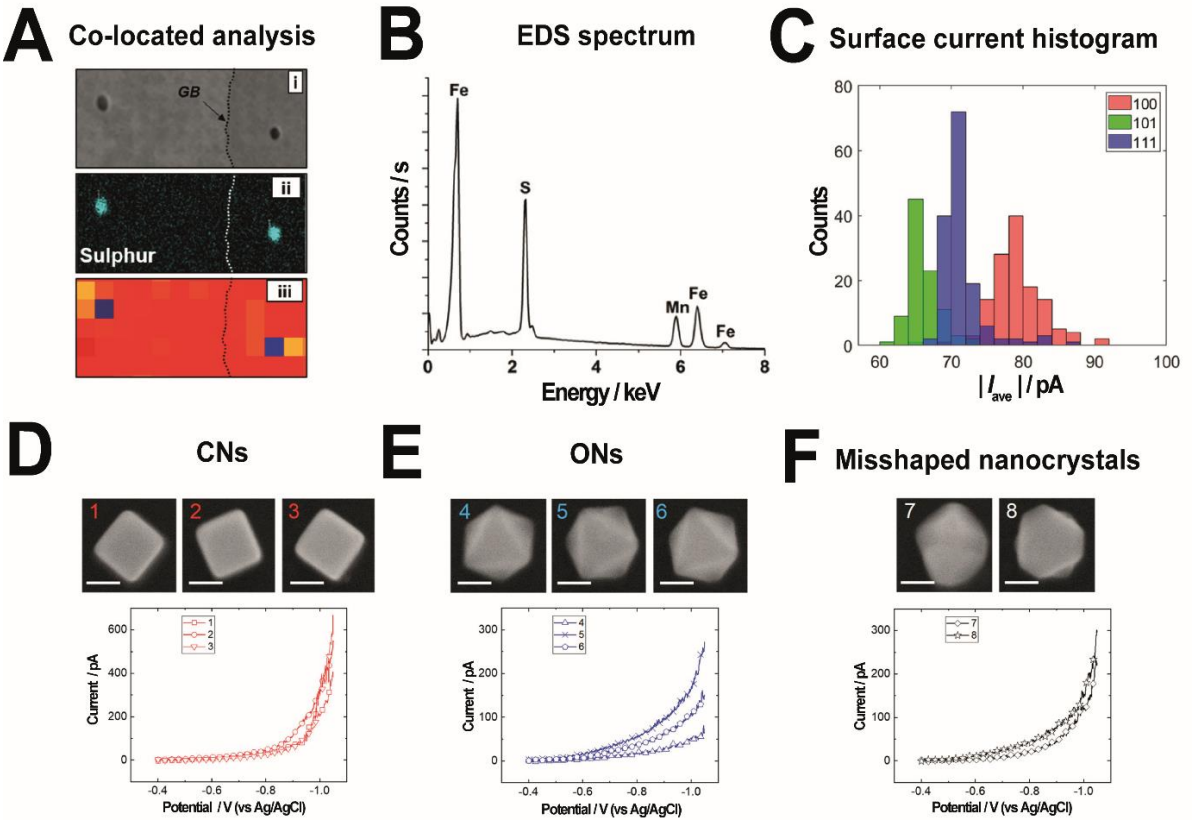

Figure 3: Electrocatalysis at inclusions and faceted nanocrystals. (A) Co-located (i) scanning electron microscope (SEM) image, (ii) energy-dispersive X-ray spectroscopy (EDS) sulfur map and (iii) electrochemical map (blue, high activity; red is low activity) obtained from SECCM, showing the hydrogen evolution reaction (HER) on low carbon steel. (B) EDS spectrum of the left inclusion shown in A. (C) Histograms of the average surface currents, I_{ave}, (measured from 7.2 to 9.8 ms during chronoamperometry at −1.337 V *vs* Ag/AgCl QRCE) from SECCM mapping on the low index grains indicated by the color bars. Reproduced from reference [9] with permission from the American Chemical Society. Note that further permissions related to the material excerpted should be directed

to the American Chemical Society. High-resolution SEM images of individual Au (D) nanocubes (NCs), (E) octahedral nanocrystals (ONs) and (F) misshaped nanocrystals (scale bar = 50 nm) with corresponding color-matched voltammograms from each nanocrystal. Numbers on SEM images correspond to legends on voltammograms. Adapted with permission from reference [15]. Copyright 2020 American Chemical Society.

2.4 Two-Dimensional Materials

An exciting category of substrates studied with SECCM are two-dimensional (2D) materials. Recent contributions have explored the edge and basal surface activity of several different materials: hexagonal boron-nitride (h-BN) [40], and transition-metal dichalcogenides (e.g., MoS_2 and WS_2) [4,41–43].

Contrary to the conclusions from macroscopic measurements that MoS_2 basal planes are catalytically inert [44], SECCM with *correlative co-located* atomic force microscopy and electron microscopy unequivocally proved that HER is catalyzed at the basal planes [4,7]. The Tafel slope and exchange current density at the basal plane was shown to be comparable to that of Au, Cu, Ni, and Co, while the exchange current density of the edge plane was an order-of-magnitude larger [4]. The high spatial resolution attainable with SECCM also facilitated the direct investigation of cracks, sulphur vacancies, layer number as well as previously unseen phenomena of aging, mechanical strain and electronic structure for HER activity on MoS_2 and WS_2 [41,42]. In similar vein, local voltammetric measurements with SECCM revealed that Au-supported h-BN exhibits about two orders of magnitude larger exchange current density than Cu-supported h-BN, highlighting the vital role of choice in metal supports for layered 2D electromaterials [40].

Towards applications of 2D materials in optoelectronics, SECCM was recently used to show that photoelectrochemical oxidation is enhanced at edge-type defect sites, compared to the basal surface at crystalline MoS_2 [43]. It was suggested that higher photocurrents at edge-type defects was due to an increased surface density of sulfur vacancies and terminal Mo-SH functional groups.

Complex Electrodes

Electrodes for practical applications continue to increase in complexity with deliberate multi-level interrelated structural and compositional manipulation [45]. SECCM has a key role to play in pinpointing the electrochemical properties of key features of such electrodes. Recently, data from nanoscale SECCM studies of conductive polymer blends was used to simulate macroscale electrochemistry, revealing that the macroscale experiment is dominated by parasitic resistance [46]. This work was able to clearly resolve the electron transfer kinetics of nanoscale conductive (poly(3-hexylthiophene, P3HT) islands compared to insulating (poly(methyl methacrylate, PMMA) domains and also highlighted the complementarity of SECCM and conducting AFM. The quality of SECCM-derived topography compared to AFM topography is evident (Figure 4A and D). In similar vein, dopamine oxidation on widely used screen printed carbon electrodes, was shown to exhibit strong dependence on the local heterogeneous microstructure of the carbon electrode [47].

With *correlative electrochemical multi-microscopy*, it has been possible to reliably and explicitly resolve the unique contribution of local structure modifications on the overall electrocatalytic activity of complex electrode materials [48–51]. An exemplar study showed that local iron-enrichment and sulphur deficiencies, as well as microscopic structures, are directly associated with enhanced HER activities on $Fe_{4.5}Ni_{4.5}S_8$ single crystals electrodes [50].

Other effects studied by SECCM include nitrogen/phosphorous co-doping on HER activity of holey graphene [49], correlation of sheet thickness and defects to photochemical reactivity of p-type WSe_2 nanosheets [51], and the relationship between local morphology of nickel (oxy)hydroxides particles and OER activity [48]. SECCM with voltammetry and galvanostatic methods revealed the effect of the morphology and thickness of ZrO_2 coating on the local cycle durability of $LiCoO_2$ thin film electrodes [52], and for a Li-air battery application, visualizing enhanced redox properties of micro-structured Li_2O_2 [53].

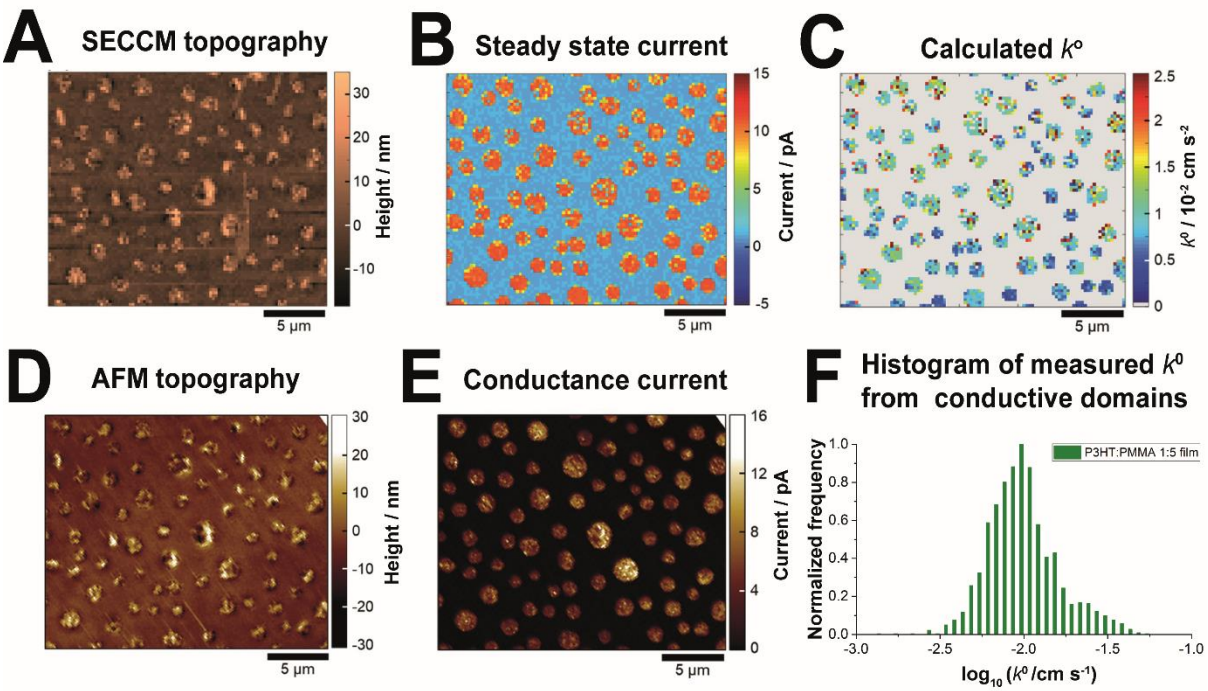

Figure 4: Correlative multi-microscopy analysis of the surface of a 1:5 P3HT:PMMA blend electrode, deposited on an ITO support. (A) Topographical and corresponding (B) synchronous electrochemical activity map recorded by SECCM. The electrochemical map (B) is at 0.74 V *vs* Ag/AgCl QRCE and is one of several hundred potential resolved images from a movie obtained with voltammetric SECCM. (C) Corresponding map of k^0 values for the ferrocenedimethanol oxidation ($FcDM^{0/+}$), calculated from the spatially resolved cyclic voltammograms from SECCM. (D) Topographical and corresponding (E) electrical conductivity maps, measured using c-AFM (bias potential = +2.0 V). (F) Histogram of

measured k^0 values for the P3HT domains in 1:5 P3HT/PMMA blend electrodes (logarithmic scale). Adapted with permission from reference [46]. Copyright 2019 American Chemical Society.

2.6 Electrodeposition and Patterning

The SECCM setup enables local delivery of species to various substrates and has recently been explored for studying electrodeposition processes to 'create' and study single NPs *in situ* [5,54]. Recent applications of this high-throughput approach have explored the electrodeposition of Pt onto carbon-coated TEM grids, which enabled co-located STEM structural analysis with single atom sensitivity [55]. This has been followed up with the use of SECCM to electrodeposit Ni_xB NPs onto liquid cell TEM chips, facilitating the subsequent *in situ* observation of the ethanol oxidation of the single particle by means of TEM movies [56]. Direct three-dimensional patterning and electrochemical characterization of arrays of conductive polymer pillars comprised of poly(3,4-ethylenedioxythiophene)-polystyrenesulfonate (PEDOT:PSS) was also successfully demonstrated [57].

3.0 Conclusion and Outlook

SECCM is coming of age and proving to be an exceptionally powerful tool for visualizing electrochemical processes across length scales at intricate heterogeneous interfaces. In this article, we have highlighted the applicability of the SECCM platform for SEE at different levels of structure-composition complexity, ranging from single particles of simple composition to characteristic features within rather complex electrodes for practical use. The understanding from these studies will enable rational design of materials for diverse applications.

For SEE studies, recent advances have seen the incorporation of various electrochemical methods into the SECCM platform, alongside correlative co-located measurements with complementary microscopy techniques. It is anticipated that in the future there will be new additions, including spectroscopic capabilities, which would boost chemical information acquired *in situ* during local SECCM experiments and provide novel insights into dynamic (electrochemical) processes at the nanoscale. It needs to be highlighted that SEE studies with SECCM can be further extended to biological and biotechnological systems and other aspects of electroanalytical chemistry. Lastly, SECCM, and related methods, are expected to play a crucial role in the elucidation of electrochemical interactions between entities, revealing associative or synergistic effects that may be important in the behavior of complex electrodes at the macroscale.

Acknowledgements

MK and PRU acknowledge support from Monash-Warwick Alliance Accelerator funding and from the Faraday Challenge Battery Characterisation (EPSRC). OJW acknowledges support from the University of Warwick Chancellor's International Scholarship. PRU is grateful to the Royal Society for a Wolfson Research Merit Award.

References and recommended reading

Papers of particular interest, published within the period of review (last 3 years), have been highlighted as:

• Paper of special interest

•• Paper of outstanding interest

[1] L.A. Baker, Perspective and prospectus on single-entity electrochemistry, J. Am. Chem. Soc. 140 (2018) 15549–15559.

[2] Y. Wang, X. Shan, N. Tao, Emerging tools for studying single entity electrochemistry, Faraday Discuss. 193 (2016) 9–39.

[3] Y. Long, P.R. Unwin, L.A. Baker, Single-entity electrochemistry: fundamentals and applications, ChemElectroChem. 5 (2018) 2918–2919.

[4] C.L. Bentley, M. Kang, F.M. Maddar, F. Li, M. Walker, J. Zhang, P.R. Unwin, Electrochemical maps and movies of the hydrogen evolution reaction on natural crystals of molybdenite (MoS_2): basal *vs.* edge plane activity, Chem. Sci. 8 (2017) 6583–6593.

[5] N. Ebejer, A.G. Güell, S.C.S. Lai, K. McKelvey, M.E. Snowden, P.R. Unwin, Scanning electrochemical cell microscopy: a versatile technique for nanoscale electrochemistry and functional imaging, Annu. Rev. Anal. Chem. 6 (2013) 329–351.

[6] N. Ebejer, M. Schnippering, A.W. Colburn, M.A. Edwards, P.R. Unwin, Localized high

resolution electrochemistry and multifunctional imaging: Scanning electrochemical cell microscopy, Anal. Chem. 82 (2010) 9141–9145.

[7] C.L. Bentley, M. Kang, P.R. Unwin, Nanoscale surface structure-activity in electrochemistry and electrocatalysis, J. Am. Chem. Soc. 141 (2018) 2179−2193.

[8] E. Daviddi, K.L. Gonos, A.W. Colburn, C.L. Bentley, P.R. Unwin, Scanning electrochemical cell microscopy (SECCM) chronopotentiometry: development and applications in electroanalysis and electrocatalysis, Anal. Chem. 91 (2019) 9229–9237.

[9] L.C. Yule, V. Shkirskiy, J. Aarons, G. West, C.L. Bentley, B.A. Shollock, P.R. Unwin, Nanoscale active sites for the hydrogen evolution reaction on low carbon steel, J. Phys. Chem. C. 123 (2019) 24146–24155.

[10] N. Ebejer, A.G. Güell, S.C.S. Lai, K. McKelvey, M.E. Snowden, P.R. Unwin, Scanning Electrochemical Cell Microscopy: A Versatile Technique for Nanoscale Electrochemistry and Functional Imaging, Annu. Rev. Anal. Chem. 6 (2013) 329–351.

[11] C.L. Bentley, M. Kang, P.R. Unwin, Scanning electrochemical cell microscopy: new perspectives on electrode processes in action, Curr. Opin. Electrochem. 6 (2017) 23–30.

[12] S.C.S. Lai, P. V. Dudin, J. V. MacPherson, P.R. Unwin, Visualizing zeptomole (electro)catalysis at single nanoparticles within an ensemble, J. Am. Chem. Soc. 133 (2011) 10744–10747.

[13] C.H. Chen, L. Jacobse, K. McKelvey, S.C.S. Lai, M.T.M. Koper, P.R. Unwin, Voltammetric scanning electrochemical cell microscopy: dynamic imaging of hydrazine electro-oxidation on platinum electrodes, Anal. Chem. 87 (2015) 5782–

5789.

[14] M.E. Snowden, A.G. Güell, S.C.S. Lai, K. McKelvey, N. Ebejer, M.A. Oconnell, A.W. Colburn, P.R. Unwin, Scanning electrochemical cell microscopy: theory and experiment for quantitative high resolution spatially-resolved voltammetry and simultaneous ion-conductance measurements, Anal. Chem. 84 (2012) 2483–2491.

•• [15] M. Choi, N.P. Siepser, S. Jeong, Y. Wang, G. Jagdale, X. Ye, L.A. Baker, Probing single-particle electrocatalytic activity at facet-controlled gold nanocrystals, Nano Lett. 20 (2020) 1233–1239.

In this work, specially engineered Au nanocrystals are individually probed for HER using the SECCM setup, resulting in a concrete statistical analysis in order to fully understand electrocatalytic activities in relation to surface structures, as well as highlighting variations in the HER activities between “apparently” identical Au nanocrystals.

[16] N.A. Payne, J. Mauzeroll, Identifying nanoscale pinhole defects in nitroaryl layers with scanning electrochemical cell microscopy, ChemElectroChem. 6 (2019) 5439–5445.

[17] P. Saha, J.W. Hill, J.D. Walmsley, C.M. Hill, Probing electrocatalysis at individual Au nanorods via correlated optical and electrochemical measurements, Anal. Chem. 90 (2018) 12832–12839.

[18] Y. Takahashi, A. Kumatani, H. Munakata, H. Inomata, K. Ito, K. Ino, H. Shiku, P.R. Unwin, Y.E. Korchev, K. Kanamura, T. Matsue, Nanoscale visualization of redox activity at lithium-ion battery cathodes, Nat. Commun. 5 (2014) 1–7.

[19] B.D.B. Aaronson, C.H. Chen, H. Li, M.T.M. Koper, S.C.S. Lai, P.R. Unwin, Pseudo-single-crystal electrochemistry on polycrystalline electrodes: visualizing activity at grains and

grain boundaries on platinum for the Fe^{2+}/Fe^{3+} redox reaction, J. Am. Chem. Soc. 135 (2013) 3873–3880.

[20] D.Q. Liu, C.H. Chen, D. Perry, G. West, S.J. Cobb, J. V. Macpherson, P.R. Unwin, Facet-resolved electrochemistry of polycrystalline boron-doped diamond electrodes: microscopic factors determining the solvent window in aqueous potassium chloride solutions, ChemElectroChem. 5 (2018) 3028–3035.

[21] L.C. Yule, E. Daviddi, G. West, C.L. Bentley, P.R. Unwin, Surface microstructural controls on electrochemical hydrogen absorption at polycrystalline palladium, J. Electroanal. Chem. (2020) DOI: 10.1016/j.jelechem.2020.114047.

[22] S.R. German, M.A. Edwards, H. Ren, H.S. White, Critical Nuclei Size, Rate, and Activation Energy of H2 Gas Nucleation, J. Am. Chem. Soc. 140 (2018) 4047–4053.

[23] Y. Wang, E. Gordon, H. Ren, Mapping the nucleation of H_2 bubbles on polycrystalline Pt via scanning electrochemical cell microscopy, J. Phys. Chem. Lett. 10 (2019) 3887–3892.

• [24] Y. Wang, E. Gordon, H. Ren, Mapping the potential of zero charge and electrocatalytic activity of metal–electrolyte interface via a grain-by-grain approach, Anal. Chem. 92 (2020) 2859–2865.

This paper demonstrates new scanning protocols for SECCM, which can be utilized to probe spatially-resolved PZC immediately prior to electrochemical reaction on polycrystalline Pt, showing high versatility of the SECCM technique as well as opening up opportunities for more detailed electrochemical characterization through SECCM.

•• [25] R.G. Mariano, K. McKelvey, H.S. White, M.W. Kanan, Selective increase in CO_2

electroreduction activity at grain-boundary surface terminations, Science (80-.). 358 (2017) 1187–1192.

R.G. Mariano, K. McKelvey, H.S. White, M.W. Kanan, Selective increase in CO_2 electroreduction activity at grain-boundary surface terminations, Science (80-.). 358 (2017) 1187–1192.

[26] L.C. Yule, C.L. Bentley, G. West, B.A. Shollock, P.R. Unwin, Scanning electrochemical cell microscopy: a versatile method for highly localised corrosion related measurements on metal surfaces, Electrochim. Acta. 298 (2019) 80–88.

[27] L.C. Yule, V. Shkirskiy, J. Aarons, G. West, B.A. Shollock, C.L. Bentley, P.R. Unwin, Nanoscale electrochemical visualization of grain-dependent anodic iron dissolution from low carbon steel, Electrochim. Acta. 332 (2020) 135267.

[28] V. Shkirskiy, L.C. Yule, E. Daviddi, C.L. Bentley, J. Aarons, G. West, Nanoscale scanning electrochemical cell microscopy and correlative surface structural analysis to map anodic and cathodic reactions on polycrystalline Zn in acid media, J. Electrochem. Soc. 167 (2020).

[29] S.M. Gateman, N.S. Georgescu, M.-K. Kim, I.-H. Jung, J. Mauzeroll, Efficient measurement of the influence of chemical composition on corrosion: analysis of an Mg-Al diffusion couple using scanning micropipette contact method, J. Electrochem. Soc. 166 (2019) C624–C630.

[30] S.E.F. Kleijn, S.C.S. Lai, T.S. Miller, A.I. Yanson, M.T.M. Koper, P.R. Unwin, Landing and catalytic characterization of individual nanoparticles on electrode surfaces, J. Am. Chem. Soc. 134 (2012) 18558–18561.

[31] B.H. Kim, J. Heo, S. Kim, C.F. Reboul, H. Chun, D. Kang, H. Bae, H. Hyun, J. Lim, H. Lee, B. Han, T. Hyeon, A.P. Alivisatos, P. Ercius, H. Elmlund, J. Park, Critical differences in 3D atomic structure of individual ligand-protected nanocrystals in solution, Science (80-.). 368 (2020) 60–67.

[32] T. Tarnev, H.B. Aiyappa, A. Botz, T. Erichsen, A. Ernst, C. Andronescu, W. Schuhmann, Scanning Electrochemical Cell Microscopy Investigation of Single ZIF-Derived Nanocomposite Particles as Electrocatalysts for Oxygen Evolution in Alkaline Media, Angew. Chemie - Int. Ed. 58 (2019) 14265–14269.

[33] J. Ustarroz, I.M. Ornelas, G. Zhang, D. Perry, M. Kang, C.L. Bentley, M. Walker, P.R. Unwin, Mobility and poisoning of mass-selected platinum nanoclusters during the oxygen reduction reaction, ACS Catal. 8 (2018) 6775–6790.

[34] A. Hamelin, M.J. Weaver, Dependence of the kinetics of proton reduction at gold electrodes on the surface cyrstallographic orientation, J. Electroanal. Chem. 223 (1987) 171–184.

[35] A.G. Güell, A.S. Cuharuc, Y.R. Kim, G. Zhang, S.Y. Tan, N. Ebejer, P.R. Unwin, Redox-Dependent spatially resolved electrochemistry at graphene and graphite step edges, ACS Nano. 9 (2015) 3558–3571.

[36] M. Dayeh, M.R.Z. Ghavidel, J. Mauzeroll, S.B. Schougaard, Micropipette contact method to investigate high-energy cathode materials by using an ionic liquid, ChemElectroChem. 6 (2019) 195–201.

[37] B. Tao, L.C. Yule, E. Daviddi, C.L. Bentley, P.R. Unwin, Correlative electrochemical microscopy of Li-ion (de)intercalation at a series of individual $LiMn_2O_4$ particles,

Angew. Chemie - Int. Ed. 58 (2019) 4606–4611.

[38] A. Kumatani, Y. Takahashi, C. Miura, H. Ida, H. Inomata, H. Shiku, H. Munakata, K. Kanamura, T. Matsue, Scanning electrochemical cell microscopy for visualization and local electrochemical activities of lithium-ion (de) intercalation process in lithium-ion batteries electrodes, Surf. Interface Anal. 51 (2019) 27–30.

[39] B.D.B. Aaronson, S.C.S. Lai, P.R. Unwin, Spatially resolved electrochemistry in ionic liquids: surface structure effects on triiodide reduction at platinum electrodes, Langmuir. 30 (2014) 1915–1919.

[40] D.Q. Liu, B. Tao, H.C. Ruan, C.L. Bentley, P.R. Unwin, Metal support effects in electrocatalysis at hexagonal boron nitride, Chem. Commun. 55 (2019) 628–631.

[41] B. Tao, P.R. Unwin, C.L. Bentley, Nanoscale variations in the electrocatalytic activity of layered transition-metal dichalcogenides, J. Phys. Chem. C. 124 (2020) 789–798.

[42] Y. Takahashi, Y. Kobayashi, Z. Wang, Y. Ito, M. Ota, H. Ida, A. Kumatani, K. Miyazawa, T. Fujita, H. Shiku, Y.E. Korchev, Y. Miyata, T. Fukuma, M. Chen, T. Matsue, High-resolution electrochemical mapping of the hydrogen evolution reaction on transition-metal dichalcogenide nanosheets, Angew. Chemie - Int. Ed. 59 (2020) 3601–3608.

[43] L.E. Strange, J. Yadav, S. Garg, P.S. Shinde, J.W. Hill, C.M. Hill, P. Kung, S. Pan, Investigating the redox properties of 2D MoS_2 using photoluminescence spectroelectrochemistry and scanning electrochemical cell microscopy, J. Phys. Chem. Lett., (2020) DOI: 10.1021/acs.jpclett.0c00769.

[44] J. Kibsgaard, Z. Chen, B.N. Reinecke, T.F. Jaramillo, Engineering the surface structure of MoS 2 toÂ preferentially expose active edge sites forÂ electrocatalysis, Nat. Mater.

11 (2012) 963–969.

[45] S. Dou, X. Wang, S. Wang, Rational Design of Transition Metal-Based Materials for Highly Efficient Electrocatalysis, Small Methods. 3 (2019) 1800211.

•• [46] E. Daviddi, Z. Chen, B. Beam Massani, J. Lee, C.L. Bentley, P.R. Unwin, E.L. Ratcliff, Nanoscale visualization and multiscale electrochemical analysis of conductive polymer electrodes, ACS Nano. 13 (2019) 13271–13284.

This paper highlights that SECCM mapping with high-spatial resolution can resolve a complex electrode configuration - a P3HT/PMMA blend - providing spatially-resolved electron transfer kinetics on the electrode and in-depth information in order to understand electrode kinetics at the macroscale electrochemistry.

[47] D. Martín-Yerga, A. Costa-García, P.R. Unwin, Correlative voltammetric microscopy: structure-activity relationships in the microscopic electrochemical behavior of screen printed carbon electrodes, ACS Sensors. 4 (2019) 2173–2180.

[48] R. Beugré, A. Dorval, L.L. Lavallée, M. Jafari, J.C. Byers, Local electrochemistry of nickel (oxy)hydroxide material gradients prepared using bipolar electrodeposition, Electrochim. Acta. 319 (2019) 331–338.

[49] A. Kumatani, C. Miura, H. Kuramochi, T. Ohto, M. Wakisaka, Y. Nagata, H. Ida, Y. Takahashi, K. Hu, S. Jeong, J. ichi Fujita, T. Matsue, Y. Ito, Chemical dopants on edge of holey graphene accelerate electrochemical hydrogen evolution reaction, Adv. Sci. 6 (2019) 1900119.

[50] C.L. Bentley, C. Andronescu, M. Smialkowski, M. Kang, T. Tarnev, B. Marler, P.R. Unwin, U.P. Apfel, W. Schuhmann, Local surface structure and composition control

the hydrogen evolution reaction on iron nickel sulfides, Angew. Chemie - Int. Ed. 57 (2018) 4093–4097.

[51] J.W. Hill, C.M. Hill, Directly mapping photoelectrochemical behavior within individual transition metal dichalcogenide nanosheets, Nano Lett. 19 (2019) 5710–5716.

[52] H. Inomata, Y. Takahashi, D. Takamatsu, A. Kumatani, H. Ida, H. Shiku, T. Matsue, Visualization of inhomogeneous current distribution on ZrO_2-coated $LiCoO_2$ thin-film electrodes using scanning electrochemical cell microscopy, Chem. Commun. 55 (2019) 545–548.

[53] E. P. E. Sharel, M. Kang, P. Wilson, L. Meng, D. Perry, A. Basile, P.R. Unwin, High resolution visualization of the redox activity of Li_2O_2 in non-aqueous media: conformal layer *vs.* toroid structure, Chem. Commun. 54 (2018) 3053–3056.

[54] K. McKelvey, M.A. O'Connell, P.R. Unwin, Meniscus confined fabrication of multidimensional conducting polymer nanostructures with scanning electrochemical cell microscopy (SECCM), Chem. Commun. 49 (2013) 2986–2988.

• [55] I.M. Ornelas, P.R. Unwin, C.L. Bentley, High-throughput correlative electrochemistry-microscopy at a transmission electron microscopy grid electrode, Anal. Chem. 91 (2019) 14854–14859.

This work presents a high-throughput SECCM-STEM platform, revealing structure-electrochemistry for the Pt electrodeposition process, and nanoscopic patterning utilizing the SECCM technique.

• [56] T. Tarnev, S. Cychy, C. Andronescu, M. Muhler, W. Schuhmann, Y.-T. Chen, A universal nano-capillary based method of catalyst immobilization for liquid cell transmission

electron microscopy, Angew. Chemie. (2020) DOI: 10.1002/ange.201916419.

This paper explores a liquid-cell TEM chip as an unusual substrate for SECCM and electrochemically fabricates Ni_xB nanocomposites onto the chip, followed by visualization in situ of structural variations on Ni_xB nanocomposites during ethanol oxidation.

[57] P. Zhang, N. Aydemir, M. Alkaisi, D.E. Williams, J. Travas-Sejdic, Direct writing and characterization of three-dimensional conducting polymer PEDOT arrays, ACS Appl. Mater. Interfaces. 10 (2018) 11888–11895.